Al$_2$O$_3$ Nanotube/Epoxy Inorganic-Organic Nanocomposites under Simulated LEO Space Environment

Joo-Hyun Han and Chun-Gon Kim [1]

[1] *Department of Aerospace Engineering, Korea Advanced Institute of Science & Technology 373-1, Kuseong-dong, Yuseong-gu, Daejeon, 305-701, Korea*

SUMMARY: In this study, low Earth orbit (LEO) space environment characteristics of Al$_2$O$_3$ nanotube reinforced epoxy matrix nanocompsites were investigated. Fabrication of Al$_2$O$_3$ nanotube/epoxy nanocomposites with different nanotube weight concentrations was made using ultra-sonication and homogenisation. Al$_2$O$_3$ nanotube/epoxy nanocomposites were tested in simulated low Earth orbit (LEO) environment. The LEO space environment simulation was characterized by high vacuum, ultraviolet (UV) radiation, and atomic oxygen (AO) atmosphere. Tensile properties, coefficient of thermal expansion, mass loss, and surface morphology of Al$_2$O$_3$ nanotube reinforced epoxy matrix composites, including un-reinforced epoxy, after the simulated LEO space environment exposure, were measured. Experimental results showed that LEO space environment characteristics of epoxy are significantly enhanced by the reinforcement of Al$_2$O$_3$ nanotubes.

KEYWORDS: Al$_2$O$_3$ nanotubes, inorganic-organic nanocomposites, space environment, low Earth orbit (LEO), atomic oxygen (AO).

INTRODUCTION

It has been known that use of polymers and polymer matrix composites (PMC's) meets the design requirements of space structures and systems, and thus they have been broadly applied as space materials. The use of these organic polymeric materials in space, however, has both positive and negative effects. Typical merits for the use are their outstanding material qualities, including light weight, high stiffness and strength, low thermal expansion, and creep resistance, as well as extraordinary optical and electrical characteristics. Regardless of these positive aspects, however, the outstanding qualities hardly maintain against the harsh space environment when they are required to operate for long term in space. The LEO space environment constituents, composed of high vacuum, UV radiation, thermal cycles, atomic oxygen (AO), charged particles, electromagnetic radiation, micrometeoroids and man made debris, terribly degrade (deteriorate) the material properties of the polymeric materials. When exposed to the severe LEO space environment, the polymers and PMC's will undergo surface erosion by AO attack, structural modification and mass loss by outgassing, fatigue cracking by thermal cycling, etc [1-2]. Thus, it is very crucial that the polymeric materials show excellent LEO space environment resistant characteristics for their efficient use in space.
Subsequently, studies to improve the protection of the polymeric materials against the hazardous space environment effects for their long-term space use have actively been made. A number of studies have been conducted to develop protective coatings on the polymers and

PMC's, as well as coating techniques for better protection. Nevertheless, the protective coatings also dramatically lose their performance if they are used in space for long period. Cracking, undercutting, and interface failures can be generated on the protective coating due to thermal cycling, collision with micrometeoroids and man-made debris, as well as its manufacturing defects, and these failures are yet to be solved.

Reinforcement of nano-sized inorganic materials to organic polymeric materials is regarded herein as a new approach to overcome the demerit of the use of organic polymers and PMC's under the destructive low Earth orbit (LEO) space environment effects. Al_2O_3 nanotube/epoxy inorganic-organic nanocomposites were proposed in the present paper. Al_2O_3 nanotubes were chosen to be the inorganic materials based on two factors: (1) Al_2O_3 nanotubes are one of metal-oxide materials which have been known to be UV tolerant and resistant to AO attack and thermal cycling [3], and widely applied for the protective coating materials against the LEO space environment effects [4], and (2) if homogeneously dispersed in polymers, nano-scaled Al_2O_3 nanotubes may efficiently enhance the resistant characteristics of insecure polymers against LEO space environment effects. After being exposed to the simulated LEO space environment, changes in mechanical and thermal properties, mass loss, and surface morphology of polymer through the reinforcement of Al_2O_3 nanotubes will be investigated and discussed in this study.

LEO SPACE ENVIRONMENT SIMULATION

A LEO space environment facility capable of simulating the characteristics of LEO environment constituents, such as high vacuum, UV radiation, thermal cycling, and atomic oxygen atmosphere was designed and manufactured to study the LEO space environment characteristics and degradation mechanisms of composite materials after being exposed to LEO space environment [2]. Figure 1 shows the LEO space environment simulation facility.

Fig. 1: LEO space environment simulation facility.

High Vacuum

Vacuum near space structures in LEO is about $10^{-6} \sim 10^{-7}$ Torr. Such high vacuum in LEO induces outgassing of polymers and PMC's and consequently results in surface contamination and changes of dimension and characteristics of the materials. A main vacuum chamber of a size of $500\phi \times 400H$(mm) was manufactured to imitate the LEO vacuum condition. The pumping system composed of both rotary pump and diffusion pump for low and high vacuums, respectively, was used to produce the chamber pressure on the order of 10^{-6} Torr at a gas extraction rate of 10 L/s.

UV Radiation

UV radiation of the wavelength of 100~200 nm is the primary electromagnetic radiation component in LEO environment [1]. Thermo-optical and mechanical properties are likely to be degraded through UV radiation exposure. The UV radiation source in the LEO simulation facility was attained using UV lamp carrying its wavelength of less than 200nm.

Thermal Cycling

Thermal cycling of $+150^\circ$C to -150°C takes place between sun-facing and shadow-facing surfaces of spacecraft operating in LEO [2]. The thermal cycling induces a mismatch in the coefficients of thermal expansion (CTE's) of the matrix and fibers and hence initiates microcracks in matrix of composite materials, which results in degradation of material characteristics of the composite materials.

The sun-facing surface temperature was simulated using a halogen lamp, set inside the chamber, while the shadow facing surface temperature was simulated using a refrigerator circulating reusable coolant through a pipe placed in the chamber. The maximum and minimum operating temperatures for the thermal cycling simulation were 100°C and -70°C, respectively. Temperature increases at a rate of approximately 5°C/min and decreases approximately 3~4°C/min; and a thermal cycle (100°C $\rightarrow$ -70°C $\rightarrow$ 100°C) takes about 64 minutes.

Atomic Oxygen

In LEO, a major neutral constituent that is very hazardous toward polymeric materials is AO. Surface erosion, mass loss, degradation in mechanical, thermal and optical properties, as well as changes in chemical compositions, of polymeric materials can be resulted through the collision with AO [1]. At an altitude of about 300 km, the densities of AO during maximum and minimum solar activities are approximately 2×10^9 and 8×10^9 atoms/cm^3, respectively. If a spacecraft orbits at the altitude with a velocity of 8 km/s, it would be encountered with AO particles with a kinetic energy of about 5 eV at the nominal AO flux ranged approximately from 10^{14} to 10^{15} atoms/cm^{2}s [3].
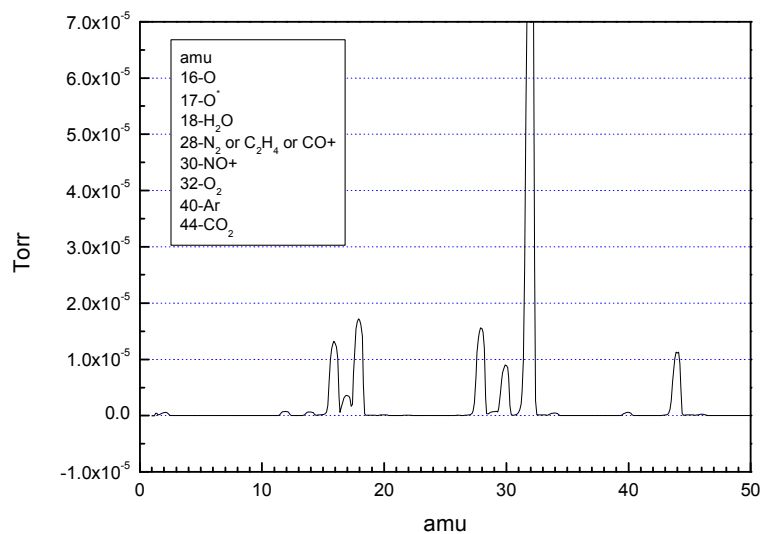

Fig. 2: Spectral mass analysis at an oxygen gas flow rate of 5.0 sccm and a RF power of 200W.

Atomic oxygen generation system equipped in the LEO simulation facility was manufactured to generate AO flux through weakly ionized remote oxygen plasma with a radio-frequency (RF) plasma source. The plasma source was mainly operated through gas (O_2 and Ar) supply and 600W, 13.56MHz RF power supply. A quadropole based residual gas analyzer (RGA), scanning mass range from 1 to 200 amu, was used to select the optimum gas-mixture flow rate and RF power, and the maximum AO density was thus obtained through controlling the gas flow rate and RF power. Figure 2 shows spectral mass analysis of the chamber while operating AO generation system at an oxygen gas flow rate of 5.0 sccm and a RF power of 200W, which provides maximum scanning of AO amongst other various gas-mixture flow rates. The maximum AO density was then determined using plasma discharge simulation, which was coded based on the rate constants for a restricted set of two body reactions of interest in modeling low-pressure oxygen discharges [5]. The estimated maximum AO density was approximately 2.264×10^{13} atoms/cm^3. Figure 3 presents densities of neutral species in plasma as a function of RF power at a gas-mixture flow rate of 5.0 sccm. The gas-mixture composition of oxygen and argon (O_2:Ar), used for the plasma discharge simulation, was 0.9:0.1 due to its coding configuration that requires both gases' flow. Comparing with the spectral mass analysis shown in Fig. 2, the estimated contents of neutral species by the plasma discharge simulation, shown in Fig. 3, were considerably similar to those by the mass analysis. Thus, it can be said that the estimated density of AO is feasible to be used in this study.

The maximum AO flux was then calculated through Eqn. 1 as follows:

$$\Gamma_N = \frac{1}{4} N \, \upsilon_N^{TH} \tag{1}$$

where Γ_N is flux of neutral species, N is density of neutral species, υ_N^{TH} is thermal velocity of neutral species. The expression of υ_N^{TH} takes the formula as shown in Eqn. 2:

$$\upsilon_N^{TH} = \sqrt{8T_N / \pi M} \tag{2}$$

where T_N is temperature of neutral species, and M is mass of neutral species [5]. The estimated temperature of atomic oxygen neutrals in the oxygen plasma was approximately 0.04 eV. The calculated maximum AO flux was approximately 4.44×10^{17} atoms/cm$^2 \cdot$s.

AO flux encountered upon the specimen in the main chamber, which was placed 341mm below the plasma source, was determined by estimating divergence angle of the AO beam. The estimation of divergence angle was conducted through measuring diameter of AO beam exposed to sample specimen as a function of distance from the orifice. Obtaining the diameters of the beam and orifice, the divergence angle and AO flux encountered upon test specimen were calculated to be approximately 6.27° and 4.50×10^{16} atoms/cm^{2}s, respectively. Regarding the nominal AO flux in LEO (250 km, $\Phi \approx 3 \times 10^{14}$ atoms/cm^{2}s), the AO generation system in the LEO simulation facility offers a suitable accelerated simulation testing of AO environment in LEO.
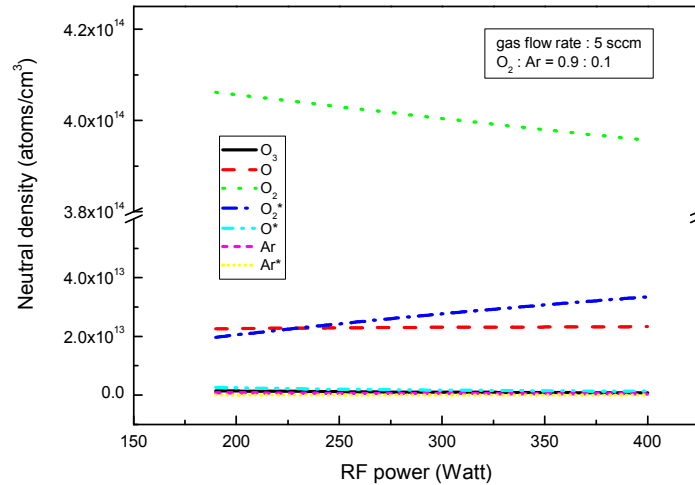
Fig. 3: Densities of neutral species in plasma vs. RF power.

FABRICATION OF NANOCOMPOSITES

Al_2O_3 nanotube/epoxy inorganic-organic nanocomposites were fabricated with different nanotube weight percent (wt.%) concentrations. Unidirectional Al_2O_3 nanotubes, synthesized by modified surfactant-templating method, were obtained from Bioplus Co., Ltd. Average length and diameter of Al_2O_3 nanotubes are 50-100 nm and 5-8 nm, respectively. TEM images of Al_2O_3 nanotubes are shown in Fig. 4. A liquid type epoxy resin (YDF-170, Kukdo Chemical Co., Korea), having low viscosity without diluents or modifiers, was obtained.
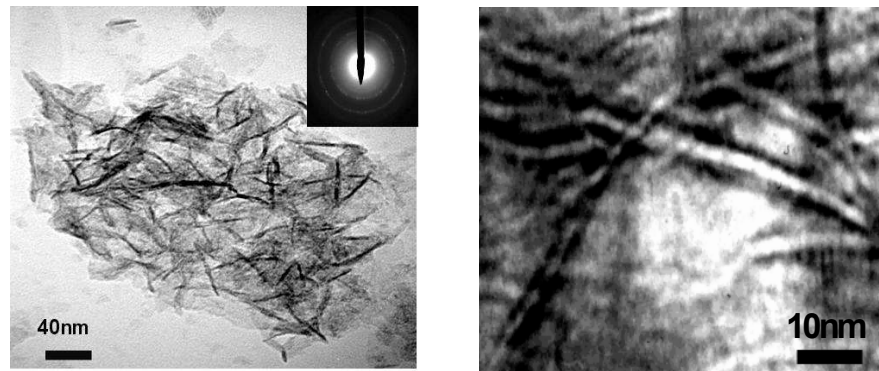

Fig. 4: TEM images of Al_2O_3 nanotubes.

Fabrication procedure for Al_2O_3 nanotube/epoxy inorganic-organic nanocomposites, consisting of three major processes, is presented as the following:

First, during the blending process, ultra-sonication was first employed to obtain uniformly dispersed Al_2O_3 nanotubes in acetone solvent. The Al_2O_3 nanotubes dispersed solvent was then mechanically mixed with epoxy resin by employing homogenization, while maintaining the temperature of the solution at 50°C. During the mechanical mixing, an appropriate amount of silane coupling agent was added to ensure strong adhesion between inorganic Al_2O_3 nanotubes and organic epoxy matrix. Both ultra-sonication and homogenization were finally employed simultaneously to attain the complete blending of Al_2O_3 nanotube/epoxy resin/acetone/silane mixture.

Second, during the evaporation process, the mixture was dried in an oven set at 70°C for over 36 hours to evaporate the acetone solvent. After being dried, the mixture solution was

mechanically mixed with hardener (DS-230, New Seoul Chem Co., Korea). The final mixture then degassed in a vacuum chamber for over 5 minutes to extract bubbles caused by the mixing.

Finally, during the curing process, the mixture was subjected to specific thermal and atmospheric curing conditions in autoclave. Finally, Al_2O_3 nanotube/epoxy nanocomposites with 0.0, 0.5, 1.0, and 2.0 wt.% concentrations, as equivalent as 0.0, 1.5, 2.9, 5.7 volume percent (vol.%) concentrations, were consequently fabricated. Figure 5 shows TEM image of 1.0 wt.% Al_2O_3 nanotube/epoxy nanocomposites, indicating that Al_2O_3 nanotubes are well dispersed in the epoxy matrix.
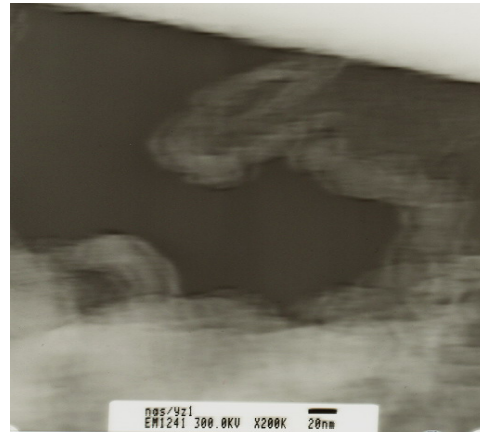

Fig. 5: TEM images of Al_2O_3 nanotube/epoxy nanocomposites with 1.0 wt.% concentration.

LEO SPACE ENVIRONMENT CHARACTERISTICS OF AL_2O_3 NANOTUBE/EPOXY NANOCOMPOSITES

Mass loss, along with mechanical or thermal property changes of Al_2O_3 nanotube/epoxy inorganic-organic nanocomposites after the synergistic LEO space environment exposure and AO exposure, were investigated and compared with those of pure epoxy to evaluate the LEO space environment characteristics of Al_2O_3 nanotube/epoxy nanocomposites. In addition, changes of material characteristics through the addition of Al_2O_3 nanotubes are investigated to evaluate their feasibility to be used as a mechanical or thermal reinforcement of polymer. All testing materials were placed in the high vacuum condition for over 24 hours, and AO exposure or LEO synergistic exposure was subsequently followed. Each exposure was conducted for 6 hours 20 minutes, so that the AO fluence of about 1.025×10^{21} atoms/cm^2 and 4 thermal cycles were made during the period.

Mass Loss

Operating in space for long-term period, polymer- or PMC-based structures significantly lose their mass through outgassing under ultra-high vacuum. The outgassing deforms the structures, causing failure of dimensional stability, and even contaminates other important structures or systems. Mass loss test for the Al_2O_3 nanotube/epoxy nanocomposites measured the total mass loss (TML) of outgassed material by the LEO space environment effects, and thus determined mass-erosion resistant characteristic of Al_2O_3 nanotube reinforced polymer matrix nanocomposites. The dimension of specimen for this test was 5×5×5 mm.
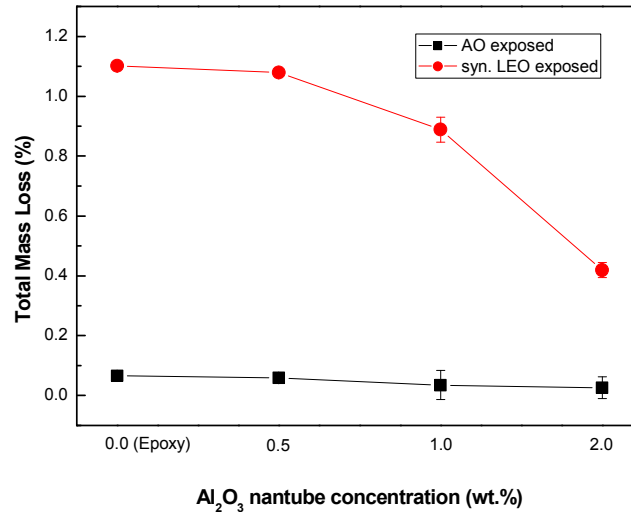
Fig. 6: TML's of Al₂O₃ nanotube/epoxy nanocomposites after AO exposure and LEO exposure.

The TML's of Al_2O_3 nanotube/epoxy nanocomposites exposed to AO and synergistic LEO environment over the aging period are shown in Fig. 6. The TML's of the nanocomposite specimens with 0.0, 0.5, 1.0 and 2.0 wt.% Al_2O_3 nanotube concentrations after AO exposure were approximately 0.124 %, 0.060 %, 0.034 %, and 0.025 %, while the TML's after synergistic LEO exposure were 1.10 %, 1.08 %, 0.89%, and 0.42 %, respectively. The mass erosion of the specimens under synergistic LEO environment was severer than that under AO effects. As a result, it was observed that under LEO space environment effects, the surface erosion (mass loss) of epoxy was significantly reduced by the reinforcement of Al_2O_3 nanotubes.

Tensile Properties

High tensile properties after space environment exposure are strongly required for space materials because it is directly associated with the damage of structures or systems in space. Tensile property test was conducted to investigate the tensile characteristics of Al_2O_3 nanotube/epoxy nanocomposites under LEO space environment effects. ASTM D638 type V was used as the tension test method.

Tensile strength and stiffness of the Al_2O_3 nanotube/epoxy nanocomposites unexposed and exposed to AO attack and synergistic LEO environment effects as a function of Al_2O_3 nanotube wt.% (vol.%) concentration are shown in Fig. 7. Prior to the space environment exposure, tensile properties of the epoxy were improved by the reinforcement of Al_2O_3 nanotubes. The maximum strength and stiffness of unexposed Al_2O_3 nanotube/epoxy nanocomposites were 74.07 MPa at 1.0 wt.% and 4.24 Gpa at 2.0 wt.% Al_2O_3 nanotube reinforcements, whereas those of epoxy were 66.14 MPa and 3.95 GPa, respectively. As compared to pure epoxy, tensile strength was enhanced 8.7 %, 12.0 %, and 7.33 % by 0.5, 1.0, and 2.0 wt.% Al_2O_3 nanotube reinforcements, and tensile stiffness was enhanced 0.0 %, 2.28 %, and 7.34 % by 0.5, 1.0, and 2.0 wt.% Al_2O_3 nanotube reinforcements, respectively.

Being exposed to AO, tensile strength and stiffness of epoxy were degraded to 63.5 Mpa and 3.85 Gpa, respectively, which indicate that epoxy suffered the severest reduction by AO attack amongst all the other Al_2O_3 nanotube/epoxy nanocomposites. The maximum tensile strength and stiffness of AO exposed Al_2O_3 nanotube/epoxy nanocomposites were also found to be 72.74 Mpa at 1.0 wt.% and 4.1 Gpa at 2.0 wt.%, indicating that tensile properties of Al_2O_3 nanotube/epoxy nanocomposites were less influenced by AO attack.
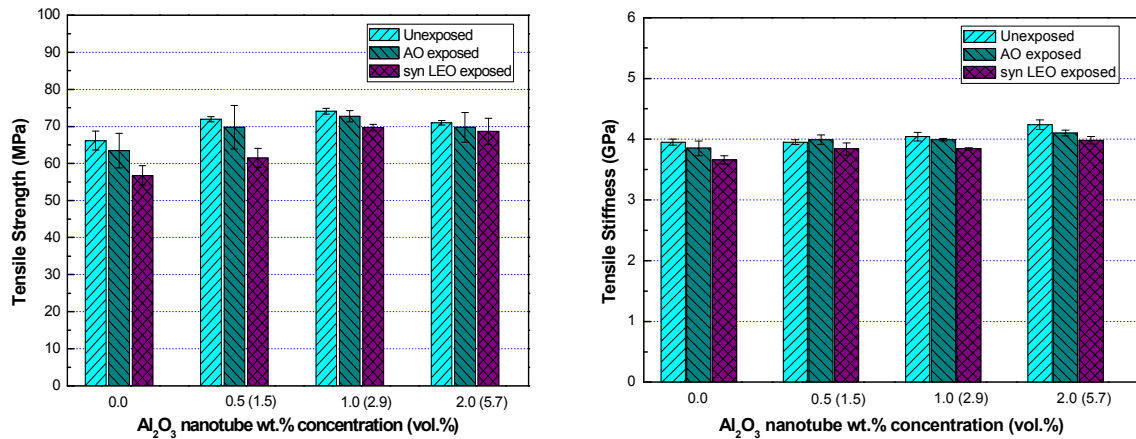
Fig. 7: Tensile strength and stiffness of Al$_2$O$_3$ nanotube/epoxy nanocomposites before and after LEO exposure.

After synergistic LEO exposure, tensile strength and stiffness of epoxy were 56.77 Mpa and 3.66 Gpa, respectively, and these were the lowest tensile properties among all the Al$_2$O$_3$ nanotube/epoxy nanocomposites. The maximum tensile strength and stiffness of synergistic LEO exposed Al$_2$O$_3$ nanotube/epoxy nanocomposites were also found to be 69.67 MPa at 1.0 wt.% and 3.98 GPa at 2.0 wt.%. Tensile properties of epoxy after being exposed to AO and synergistic LEO environment were significantly increased as reinforced amount of Al$_2$O$_3$ nanotubes increases. However, it is observed that excessive amount of Al$_2$O$_3$ nanotubes beyond a certain weight concentration reduces the tensile characteristics of AO and LEO exposed Al$_2$O$_3$ nanotube/epoxy nanocomposites. In addition, tensile strength of 1.0 wt.% Al$_2$O$_3$ nanotube reinforced nanocomposites after synergistic LEO space environment exposure is greater than that of unexposed pure epoxy, and tensile stiffness of 2.0 wt.% Al$_2$O$_3$ nanotube reinforced nanocomposites after LEO exposure is greater than that of unexposed epoxy. It can thus be said that Al$_2$O$_3$ nanotube/epoxy nanocomposites can be used in LEO space, possessing greater materials properties than pure epoxy. Consequently, LEO space environment resistant characteristics of typical polymeric materials, epoxy, can be significantly enhanced by the reinforcement of small weight of Al$_2$O$_3$ nanotubes.

Coefficient of Thermal Expansion

As an essential material property for space use, low thermal expansion of polymers and PMC's for space use is strongly required to maintain its dimensional stability under severe thermal changes [6]. Thermal property test, measuring coefficients of thermal expansion (CTE's) of Al$_2$O$_3$ nanotube/epoxy nanocomposites, was performed to determine if the reinforcement of Al$_2$O$_3$ nanotubes enhances thermal properties of polymers or PMC's and how much Al$_2$O$_3$ nanotube/epoxy nanocomposites maintain their thermal characteristics after the LEO space environment exposure. The dimension of specimen for the test is 35 mm in width, 70 mm in length, and 5 mm in thickness.

Figure 9 show CTE's of Al$_2$O$_3$ nanotube/epoxy nanocomposites before and after the LEO space environment exposure. Without the LEO space environment effects, epoxy showed the highest coefficient of thermal expansion, whereas 1.0 wt.% Al$_2$O$_3$ nanotube/epoxy nanocomposite showed the lowest coefficient. It is seen that Al$_2$O$_3$ nanotube reinforced epoxy matrix composites carried much less thermal expansion under high thermal environment. At 75 $^{\circ}$C, the CTE's of 0.0 (epoxy), 0.5, 1.0, and 2.0 wt.% Al$_2$O$_3$ nanotube/epoxy nanocomposites were 87.3, 42.7, 39.6, and 55.9 ppm $^{\circ}$C^{-1}, respectively. It can be said from

Fig. 9 that through the reinforcement of Al_2O_3 nanotubes, epoxy began possessing the enhanced thermal property, such as low CTE.

After being exposed to the LEO space environment effects, as similar as unexposed composites, Al_2O_3 nanotube reinforced epoxy matrix nanocomposites showed much less CTE's than epoxy. However, CTE's of Al_2O_3 nanotube/epoxy nanocomposites were reduced after the LEO exposure. At 75 ^oC, 84.7, 33.7, 37.6, and 38.7 ppm $^oC^{-1}$, of epoxy, 0.5, 1.0, and 2.0 wt.% Al_2O_3 nanotube/epoxy nanocomposites were observed, respectively. It can be said that epoxy used in this study showed reduced CTE under LEO effects, and through the reinforcement of Al_2O_3 nanotubes, epoxy began possessing more reduced CTE, showing improved thermal property.
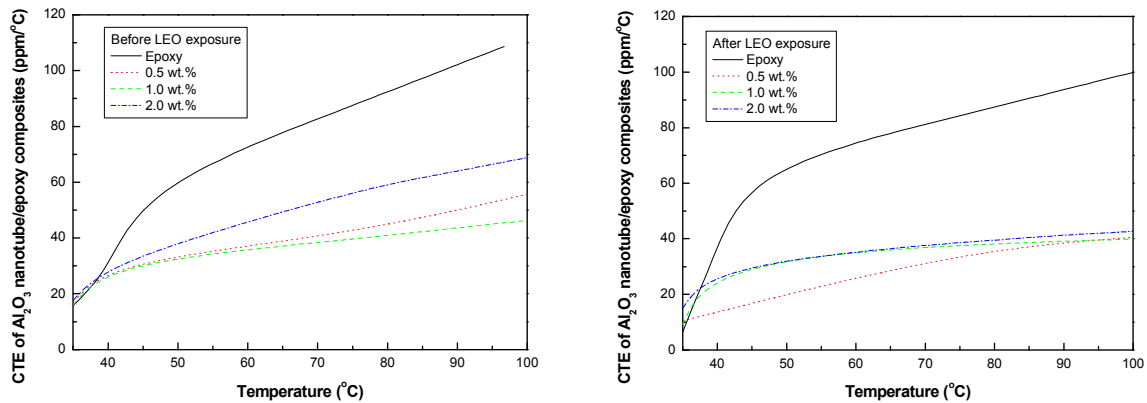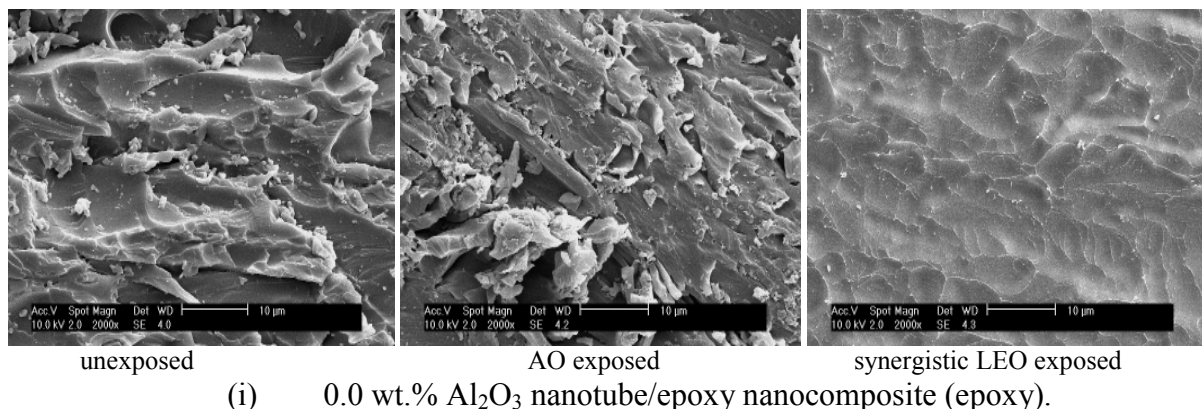

Fig. 9: CTE's of Al_2O_3 nanotube/epoxy nanocomposites vs. temperature.

Surface Morphology

Surface morphologies of the unexposed, only AO exposed, and synergistic LEO space environment exposed Al_2O_3 nanotube/epoxy nanocomposites with 0.0 and 1.0 Al_2O_3 nanotubes wt.% concentrations were taken by SEM (2000x), in order to observe the changes of surface appearance, as shown in Fig. 10. Observing the surface morphologies of Al_2O_3 nanotube/epoxy nanocomposites before and after AO exposure, it is seen that the surface of epoxy matrix was less significantly eroded. However, the whole surface of epoxy after being exposed to the synergistic LEO effects, as shown in Fig. 10, rather seemed to be swept away, which can be the main cause of the greatest reduction in mass and tensile properties after the LEO exposure. In contrast, 1.0 wt.% Al_2O_3 nanotube reinforced epoxy matrix composites showed just little erosion in its surface after AO exposure; moreover, after the LEO exposure, as compared to epoxy, it seemed to be less swept, which prove the enhanced material characteristics of Al_2O_3 nanotube reinforced epoxy matrix composites under LEO space environment effects.

unexposed   AO exposed   synergistic LEO exposed
(i)   0.0 wt.% Al_2O_3 nanotube/epoxy nanocomposite (epoxy).

unexposed   AO exposed   synergistic LEO exposed

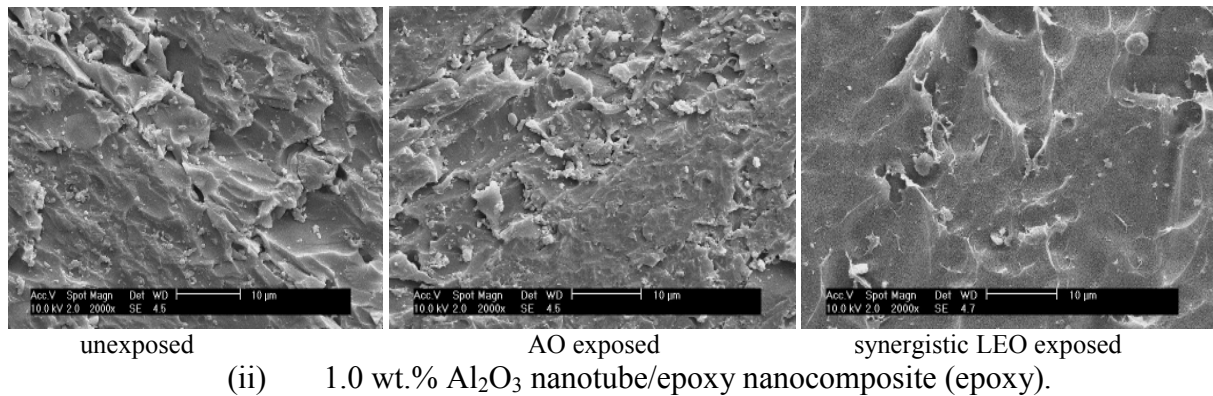(ii)   1.0 wt.% Al_2O_3 nanotube/epoxy nanocomposite (epoxy).

Fig. 10: SEM surface morphologies of Al_2O_3 nanotube/epoxy nanocomposites before and after AO exposure and synergistic LEO environment exposure.

CONCLUSION

In this study, Al_2O_3 nanotube/epoxy inorganic-organic nanocomposites were fabricated with 4 different nanotube wt.% concentrations, and their LEO space environment characteristics were investigated. Mass loss, tensile properties, CTE of Al_2O_3 nanotube reinforced epoxy matrix composites and pure epoxy, after the LEO space environment exposure, were measured, and compared with those of unexposed ones. Mass loss and CTE were reduced, and tensile properties were enhanced by the reinforcement of Al_2O_3 nanotubes. However, increasing amount of Al_2O_3 nanotubes beyond a certain weight concentration can degrade these properties. Consequently, it can be said that the reinforcement of Al_2O_3 nanotubes significantly enhanced the LEO resistant characteristics of epoxy.

REFERENCES

1.   Tennyson, R.C., "Composites in Space - Challenges and Opportunities," *Proceedings of ICCM-10*, 1995.

2.   Han, J.H., and Kim, C. J., "Low Earth Orbit Space Environment Simulation and Its Effects on Graphite/Epoxy Composites," *Composite Structures*, in press.

3.   Kleiman, J.I., Iskanderova, Z.A., Perez, F.J., and Tennyson, R.C., "Effects of Compaction on the Stiffness and Strength of Plain Weave Fabric RTM Composites", *Journal of Composite Materials*, Vol. 30, No. 11, 1996, pp. 1210-1247.

4.   Banks, B.A., Snyder, A., Miller, S.K., and Groh, K.K., "Atomic Oxygen Undercutting of Protected Polymers in Low Earth Orbit," *Journal of Spacecraft and Rockets*, Vol. 41, No. 3, 2004, pp. 335-339.

5.   Lieberman, M.A., and Lichtenberg, A.J., *Principles of Plasma Discharges and Material Processing*, John Wiley & Sons, New York, 1994.

6.   Tompkins, S.S., "Thermal Expansion of Selected Graphite-Reinforced Polyimide-, Epoxy-, and Glass-Matrix Composites," *International Journal of Thrmophysics*, Vol. 8, No. 1, 1987, pp. 119-132.